# Composite Rotor Blade Design Optimization for Vibration Reduction with Aeroelastic Constraints

GUO Jun-xian, XIANG Jin-wu

*(Institute of Aircraft Design, Beijing University of Aeronautics and Astronautics, Beijing, 100083, China)*

**Abstract:** The paper presents an analytical study of the helicopter rotor vibratory load reduction design optimization with aeroelastic stability constraints. The composite rotor blade is modeled by beam type finite elements, and warping deformation is taken into consideration for 2-dimension analysis, while the one-dimension nonlinear differential equations of blade motion are formulated via Hamilton's principle. The rotor hub vibratory loads is chosen as the objective function, while rotor blade section construction parameter, composite material ply structure and blade tip swept angle as the design variables, and autorotation inertia, natural frequency and aeroelastic stability as the constraints. A 3-bladed rotor is designed, as an example, based on the vibratory hub load reduction optimization process with swept tip angle and composite material. The calculating results show a 24.9%-33% reduction of 3/rev hub loads in comparison with the base-line rotor.

**Key words:** vibration reduction optimization; aeroelastic constraint; composite rotor blade design

带气弹稳定性约束的复合材料桨叶减振优化设计. 郭俊贤, 向锦武. 中国航空学报(英文版), 2004, 17(3): 152-158.

摘 要: 研究以降低直升机旋翼激振力为目标的复合材料桨叶结构动力学减振优化设计, 分析了桨叶结构特性及桨尖后掠角等参数对 *N* 次/转旋翼桨毂振动载荷的影响。在建立的桨叶二维结构特性有限元分析方程中, 计入了桨叶剖面翘曲变形的影响, 并利用哈密尔顿原理推导了旋翼桨叶的一维非线性运动微分方程。以桨毂交变载荷为目标函数, 直接以复合材料桨叶典型剖面构造节点数据、铺层设计参数和桨尖后掠角等为设计变量, 引入桨叶挥舞惯量、固有频率和气弹稳定性约束, 进行旋翼的动力学优化设计, 并结合 3 片桨叶旋翼的设计进行了算例分析, 优化结果使 3 次/转的桨毂载荷降低了 24.9%~33%。

关键词: 减振优化设计; 气弹约束; 复合材料旋翼桨叶设计

文章编号: 1000-9361(2004)03-0152-07 中图分类号: V212.4 文献标识码: A

As one of the major vibration sources, the helicopter rotor has gained severe attentions for a long time in foreign researches, and a lot of efforts had been given to achieve helicopter vibration reduction by decreasing the vibratory loads from the rotor. The design optimizations mainly focused on rotor blade dynamic characteristics (including natural frequency and mode shape), rotor hub vibratory load (especially *N*/rev load) and hub vibration level. The rotor blade weight, autorotation inertia and aeroelastic stability were usually selected as optimization objective functions or constraints, while blade mass and/or stiffness span-wise distributions, aerodynamic parameters (such as blade platform, pre-twist law, and tip shape, *etc.*), as well as the ply angle of composite lay-ups in blade cross-section structures, were used as design variables in optimizations[1]. However, the blade structural models adopted in these researches were awfully simplified even in the latest reference paper[2], and for the sake of easy optimization process, a simple two-box beam section model was chosen as the optimizing composite blade, which was actually much different from the real designed blades, so as to lead to a result that would be far from the real helicopter situation.

Received date: 2003-07-10; Revision received date: 2003-12-08

Up till now, only a few references were reported with composite blade section ply structures (including ply angle as well as other ply shape parameters) as design variables, and meanwhile the $N$/rev hub vibratory load as objective function, with aeroelastic stability constraints. This paper presents, in accord with the above descriptions, the effort of structural optimization of composite rotor blade with C-spar and D-shape-torsion-box section to minimize the $N$/rev vibratory hub load. The typical blade cross-section with out-of-plane warping is included in the blade model. The blade section structural parameters are calculated with 2D FEM, and the nonlinear equations of blade motion are derived using Hamilton's principle for aeroelastic analysis[3-5]. A 3-blade rotor is considered for optimization design with 3/rev vibratory hub vertical shear force as objective function, and blade dynamic frequency, aeroelastic stability and autorotation inertia as constrains, while blade cross-section composite ply parameter and tip swept angle as design variables. A reduction of 24.9%-33% in 3/rev vertical hub shear can be obtained from optimization in comparison with the initial design as for baseline rotor model.

## 1 Blade Structural Model and Formulation of Equations of Motion

The rotor blade is described as an elastic beam with constant rotating speed $\Omega$. A main current part and a tip part are divided on the blade, and an angle $\Lambda_s$ is used to define the tip sweep. The basic hypotheses used are listed in the following:

(1) For 2D structural property analysis: whole blade section movement with additional 3D warping, expressed in displacement;

(2) For one-dimension aeroelastic analysis: blade with a nonlinear moderate deflection, rigid cross-section, isolated homogeneous rotating beam;

(3) Blade with non-uniform mass and stiffness distributions, nonlinear twist and small precone;

(4) Blade with little torsion deformation, and chord length far less than blade radius.

The rotor non-rotating coordinates $\boldsymbol{e}_H(\hat{i}_{nr}, \hat{j}_{nr}, \hat{k}_{nr})$ and shown coordinates $\boldsymbol{e}_{Hr}(\hat{i}_r, \hat{j}_r, \hat{k}_r)$ are shown in Fig. 1.

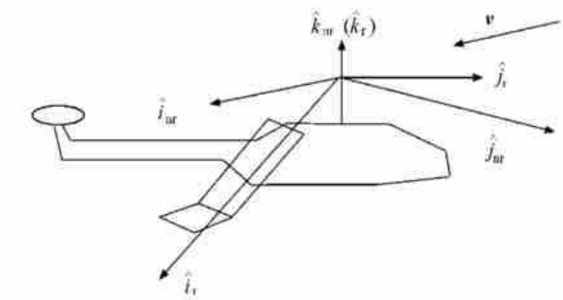


Fig. 1 Coordinates of rotor system
(footnotes "r" and "nr" stand for rotating and non-rotating, respectively)

### 1.1 Blade structural analysis

Arbitrary cross-sectional shape and anisotropic composite material behavior are considered in blade structural 2D FEM analysis[3-5]. The displacement of any point in the cross-section can be written as

$$\boldsymbol{u} = \begin{Bmatrix} w_0 + y\theta_x - x\theta_y + g_z \\ u_0 - y\theta_z + g_x \\ v_0 + x\theta_z + g_y \end{Bmatrix} \tag{1}$$

where $\boldsymbol{u} = \{w \quad u \quad v\}^T$ is the displacement of any point in section, $\boldsymbol{s}_0 = \{w_0 \quad u_0 \quad v_0\}^T$ is the translation of one section as a whole, $\theta_0 = \{\theta_z \quad \theta_x \quad \theta_y\}^T$ is angular displacement, and $\boldsymbol{g} = \{g_z \quad g_x \quad g_y\}^T$ is the elastic displacement, while $g_x$ and $g_y$ are the warpings in the section and $g_z$ is the warping out of the section (plane). According to the relationship of stress-displacement, the following is obtained,

$$\varepsilon = \begin{Bmatrix} w'_0 + y\theta'_x - x\theta'_y + g'_z \\ u'_0 - \theta_y - y\theta'_z + g'_x + \dfrac{\partial g_z}{\partial x} \\ v'_0 + \theta_z + x\theta'_z + g'_y + \dfrac{\partial g_z}{\partial y} \\ \dfrac{\partial g_x}{\partial x} \\ \dfrac{\partial g_y}{\partial y} \\ \dfrac{\partial g_y}{\partial x} + \dfrac{\partial g_x}{\partial y} \end{Bmatrix} \tag{2}$$

And then, based on minimum potential energy principle, the equilibrium equation with its conditions of the section can be derived. From one of the specific solution to the equations the inverse of the stiffness matrix will be obtained with unit load method. The stiffness matrix as well as other section properties can be resulted.

### 1.2 Equations of blade motion

The blade is divided into several beam elements while a single finite element is used for the swept tip. The equation of blade motion can be deduced by application of Hamilton's principle in discretized form:

$$\int_{t_1}^{t_2}\sum_{i=1}^{n}[\delta U_i - \delta T_i - \delta W_i]\mathrm{d}t = 0 \qquad (3)$$

where $n$ is the total number of finite elements, $\delta U_i$, $\delta T_i$ and $\delta W_i$ are the variations of strain energy, kinetic energy and virtual work of external load, respectively, of element $i$. The final form of the equation is as following:

$$\boldsymbol{M}\ddot{y} + \boldsymbol{C}\dot{y} + \boldsymbol{K}y = \boldsymbol{F} \qquad (4)$$

### 1.3 Analysis of rotor aeroelastic response and stability

The modeling of rotor blade aeroelastic analysis is to build the dynamic equation of motion with finite element method and get the final form as shown in formula (4). Usually this equation of motion can be written as

$$\boldsymbol{M}\ddot{y} + \boldsymbol{C}(\psi)\dot{\boldsymbol{y}} + \boldsymbol{K}(\psi)\boldsymbol{y} = \boldsymbol{F}(\psi, \boldsymbol{y}, \dot{\boldsymbol{y}}) \qquad (5)$$

Here, $\boldsymbol{M}$ and $\boldsymbol{C}(\psi)$ include the effects of aerodynamic and inertial forces, $\boldsymbol{K}(\psi)$ include the effects of aerodynamic inertial force and structures, while the effects of all nonlinear terms and excitation forces are included in $\boldsymbol{F}(\psi, \boldsymbol{y}, \dot{\boldsymbol{y}})$.

The solution of blade aeroelastic response analysis is based on Floquet theory with status transmission matrix. The Eq. (5) are transferred into status equations in status space and the nonlinear terms are locally linearized, until the blade steady response is obtainee from irritations of the equations.

As for blade aeroelastic stability analysis, Eq. (5) is linearized about static equilibrium position, and the stability of the blade is obtained from the solution of a standard eigenvalue problem. And for isolated rotor blade, it will be

$$\boldsymbol{M}_b\ddot{\boldsymbol{q}}_{b0} + \boldsymbol{C}_b\dot{\boldsymbol{q}}_{b0} + \boldsymbol{K}_b\boldsymbol{q}_{b0} + \boldsymbol{K}_{b\lambda}\lambda_0 =$$

$$\boldsymbol{F}_b(\boldsymbol{q}_{b0}, \dot{\boldsymbol{q}}_{b0}, \ddot{\boldsymbol{q}}_{b0}) \qquad (6)$$

$$\boldsymbol{M}_b\Delta\ddot{\boldsymbol{q}}_b + \boldsymbol{C}_b\Delta\dot{\boldsymbol{q}}_b + \boldsymbol{K}_b\Delta\boldsymbol{q}_{b0} =$$

$$\Delta\boldsymbol{F}_b(\boldsymbol{q}_{b0}, \dot{\boldsymbol{q}}_{b0}, \ddot{\boldsymbol{q}}_{b0}, \Delta q_b, \Delta\dot{q}_b, \Delta\ddot{q}_b) \qquad (7)$$

where,

$$\Delta\boldsymbol{F}_b = \frac{\partial\boldsymbol{F}_b}{\partial\boldsymbol{q}_b}\Big|_{b0}\Delta\boldsymbol{q}_b + \frac{\partial\boldsymbol{F}_b}{\partial\boldsymbol{q}_b}\Big|_{b0}\Delta\dot{\boldsymbol{q}}_b + \frac{\partial\boldsymbol{F}_b}{\partial\boldsymbol{q}_b}\Big|_{b0}\Delta\ddot{\boldsymbol{q}}_b \qquad (8)$$

From the result of eigenvalue problem analysis with Floquet theory, it gives $\lambda_k = \xi_k + \mathrm{i}\omega_k$. If the real part $\xi_k < 0$, then the stability is confirmed.

## 2 Hub Vibratory Load Optimization

The hub vibratory loads can be obtained by the given aeroelastic response analysis. The force integral is used to form blade root force from distributed components in rotating coordinats, and transferred to the non-rotating system as hub loads. In this paper the $N$/rev vibratory hub loads, which are the determinant components for rotor vibration reduction, are calculated and then optimized.

### 2.1 Description of blade structure and design variables

The composite blade is constructed with C-spar and D-shape torsion box, which is one of the popular engineering structural forms, and the blade typical cross-section is demonstrated in Fig. 2.

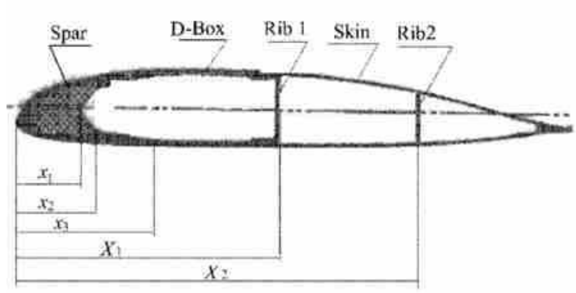


Fig. 2 Blade typical cross-sectional structure and parts of ply design variables

(1) Design variables of blade typical cross-section

The main structural parameters of blade current part are chosen as design variables of cross-section:

$$\boldsymbol{V}_1 = (x_1, x_2, y_2, x_3, X_1, X_2) \qquad (9)$$

and $\boldsymbol{V}_2 = (n_1, m_1, n_2, m_2, \ldots n_L, m_L)$ (10)

where $x_1$, $x_2$, $y_2$ and $x_3$ are shape point coordinates of C-spar, $X_1$ and $X_2$ are positions of forward and aft ribs of D-shape torsion box; $m_I$ and $n_I$ ($I = 1, 2, \ldots L$) are material codes and ply numbers of skin and torsion box, respectively, Here $m_I$ and $n_I$ are treated as discrete variables, while the values can only be chosen in a set of arrangemens relative to the blade section structure. The materials and ply angles of the forward and aft ribs are supposed to be the same as those of the D-box.

The continuity of section between different blade elements is linearly connected as

$$V_I = \xi V_{I1} + (1 - \xi) V_{I2} \qquad (11)$$

where, $V_{I1}$ and $V_{I2}$ are section design variables, and the second footnote stands for the left (−) or right (+) side view of the same section.

(2) Design variables of concentrated weight

The blade frequency tuning and mass balancing weights are defined by:

$$\boldsymbol{V}_3 = (M_1, Z_1, \ldots M_B, Z_B) \qquad (12)$$

where $M_S$ and $Z_S$ ($S = 1, 2, \ldots B$) are the mass value and its spanwise position, respectively, while $N_B$ is the number of weights used.

(3) Design variables of tip sweep angle The blade tip is defined by swept angle $\Lambda_S$ and its position $Z_{\Lambda_S}$, tapered ratio $R_T$ and position $Z_{RT}$, *i. e*,

$$\boldsymbol{V}_4 = (\Lambda_S, Z_{\Lambda S}, R_T, Z_{RT}) \qquad (13)$$

### 2.2 Model of optimization analysis[6-8]

(1) Objective functions

$$f(D) = K_F[(F_{x,N})^2 + (F_{y,N})^2 + (F_{z,N})^2]^{1/2} + K_M \cdot [(M_{x,N})^2 + (M_{y,N})^2 + (M_{z,N})^2]^{1/2} \qquad (14)$$

or

$$f(D) = K_1 F_{x,N} + K_2 F_{y,N} + K_3 F_{z,N} \qquad (15)$$

where $F$ and $M$ stand for the hub force and moment, with footnotes $x$, $y$ and $z$, to the six components; while $K_F$, $K_M$, $K_1$, $K_2$ and $K_3$ are weighted factors.

(2) Constraints

①Frequency $\omega_i$: the first $m$-th mode frequencies will meet the limits as following:

$$g_{i,U}(D) = \frac{\omega_i}{\omega_{i,U}} - 1 \leqslant 0$$

$$i = 1, 2, \cdots, m \qquad (16)$$

$$g_{i,L}(D) = 1 - \frac{\omega_i}{\omega_{i,L}} \leqslant 0$$

$$i = 1, 2, \cdots, m \qquad (17)$$

where $\omega_{i,U}$ and $\omega_{i,L}$ are the upper and lower limits of the acceptable blade frequencies, and in this research the mode number $m$ is set as 7.

②Aeroelastic stability: the following constrains are given:

$$g(D) = \xi_k + \varepsilon_k \leqslant 0, \quad k = 1, 2, \cdots, M \qquad (18)$$

where $\xi_k$ is the real part of eigenvalue of $k$-th mode in hover, and $\varepsilon_k$ is the acceptable minimum damping for $k$-th mode in hover. $M$ is the number of modes.

The aeroelastic stability analysis in forward flight is not included in the optimization process, but is checked after when the optimized design comes out to confirm that there is no stability problem.

③Autorotation inertia $I_b$: the following constrains are given:

$$g(D) = 1 - \frac{I_b}{I_0} \leqslant 0 \qquad (19)$$

where $I_0$ is the minimum target value necessary for helicopter autorotation.

## 3 Results and Discussion

The results presented in this section are for three bladed sphere-flex rotor, in which the blade current (airfoil) part is divided into 4 elements, with the blade tip (10% of blade radius) as a single finite element. The composite blade cross-section is designed with C-spar and two cells. The structural properties of blade root part, as well as the hub components are given in real values. The design optimization is performed for 3/rev hub loads at advancing ratio $\mu = 0.3$ in level flight.

Three cases are conducted for optimization from the initial design:

(1) The structural parameters such as cross-sectional properties, ply structure and generalized weight are used for design variables to minimize the 3/rev hub loads;

(2) The blade tip sweep parameters are used for design variables to minimize the 3/rev hub loads;

(3) Based on the optimization of the first

case, the blade tip sweep parameters are used for design variables, to minimize the 3/rev loads, and the tip sweep angle value can be ranged from $-4°$ to $+28°$. A $4°$ step is set in the presented example, for higher efficiency.

The hub vertical shear force is chosen as the optimization objective function, *i.e.*, in Eq. (15), put $K_1 = 1.0$, $K_2 = K_3 = 0$, and get

$$f(D) = F_{z,N} \quad (20)$$

The blade frequency limitations are listed in Table 1, while the minimum autorotation inertia for single blade $I_0 = 334\ \text{kg}\cdot\text{m}^2$.

**Table 1 Blade frequency limitations($s^{-1}$)**

| Order of mode | 1 | 2 | 3 | 4 | 5 | 6 | 7 |
|---|---|---|---|---|---|---|---|
| Lower limitation | 20.00 | 41.50 | 88.88 | 169.68 | 169.68 | 214.12 | 286.80 |
| Upper limitation | 25.00 | 45.00 | 111.10 | 193.92 | 193.92 | 234.32 | 303.00 |

For aeroelastic stability, the first mode of flapping, lead-lag and torsion are chosen as constraints, and for convenient in calculation, $\varepsilon_k$ in Eq. (18) is set as 0.02 for each mode (it is possible to set one value for different modes).

As for reference, a helicopter rotor blade in service is analyzed, with the related parameters listed in Table 2, while Tables 3 and 4 present the initial design and optimized results, respectively.

**Table 2 Parameters of reference rotor blade**

| General parameters | Blade |
|---|---|
| Diameter 10.69m | Chord 0.35 m |
| Number of blades 3 | Airfoil OA212/OA209 |
| Speed 386 r/min | Pre-twist -12°/R |
| Disk load 22.344N/m$^2$ | Dynamic frequency : |
| Rotor hub: | 1st-4th flapping modes (Ω): |
| Hub radius 0.565m | 1.032, 2.53, 4.58, 7.12 |
| Flapping hinge offset 0.205m | 1st-2th lead-lag modes (Ω): |
| Lead-lag hinge offset 0.205m | 0.55, 4.66 |
| Pitch-flap coupling parameter $k_\beta = 0$ | 1st torsion mode (Ω) : |
| Precone 3.5° | 5.11 |

In case 1, the optimization of blade mass and stiffness spanwise distributions resulted from blade section ply structures gives 12% and 4% reductions of 3/rev hub vertical shear force, in comparison with the initial design and reference rotor blade, respectively. In case 2, the optimization of blade tip sweep angle gives 24.9% and 19.6% reductions of 3/rev hub vertical shear force, in comparison with the initial design and reference rotor blade, respectively. In case 3, the combined optimization resulted from ply organization and tip sweep angle ($\Lambda_s = 20°$) gives 33% and 21% reductions of 3/rev hub vertical shear force, in comparison with the initial design and reference rotor blade, respectively. The comparisons are shown in Fig. 3, and the other components of 3/rev hub loads, which are not included in the objective function, are also figured out in Fig. 4 and Fig. 5.

**Table 3 Comparison of initial design and optimized result (blade design variables)**

| No | Design variable | | | Initial value | Optimized value |
|---|---|---|---|---|---|
| 1 | Spar shape points | | $x_1$/mm | 48.0 | 45.5 |
| | | | $x_2$/mm | 42.0 | 40.5 |
| | | | $y_2$/mm | 13.0 | 12.0 |
| | | | $x_3$/mm | 39.0 | 38.5 |
| 2 | Rib position | | $X_1$/mm | 180 | 165 |
| | | | $X_2$ | Only one rib designed | |
| 3 | Skin ply | 0° | Number of materials $n_L$ | 3 | 1 |
| | | | Number of plies $m_L$ | $[1/2/2]_s$ | $[2]_s$ |
| | | ±45° | Number of materials $n_L$ | 2 | 2 |
| | | | Number of plies $m_L$ | $[4/4]_s$ | $[2/2]_s$ |
| 4 | D-box ply | ±45° | Number of materials $n_L$ | 2 | 2 |
| | | | Number of plies $m_L$ | $[4/6]_s$ | $[6/4]_s$ |
| 5 | Concentrated | | Mass/kg | 1.2 | 0.5 |
| | | | Acting position/% | 50 Radius | 45 Radius |

**Table 4 Blade frequency after optimization**

| Mode | $\omega_{\beta 1}$ | $\omega_{\beta 2}$ | $\omega_{\beta 3}$ | $\omega_{\beta 4}$ | $\omega_{\zeta 1}$ | $\omega_{\zeta 2}$ | $\omega_{\phi 1}$ |
|---|---|---|---|---|---|---|---|
| $s^{-1}$ | 41.693 | 98.576 | 176.144 | 292.092 | 22.22 | 187.052 | 220.584 |
| ω/Ω | 1.03 | 2.44 | 4.36 | 7.23 | 0.55 | 4.63 | 5.46 |

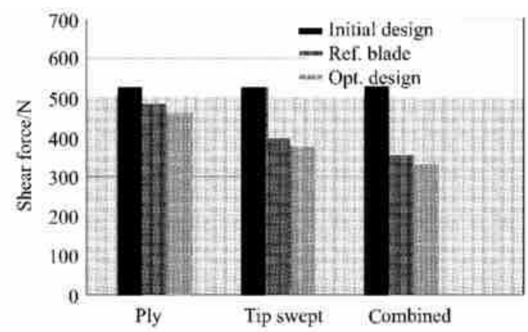


Fig. 3 3/rev optimized hub vertical shear forces

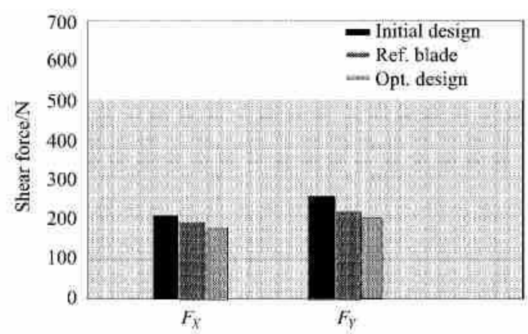


Fig. 4 3/rev other hub shear forces

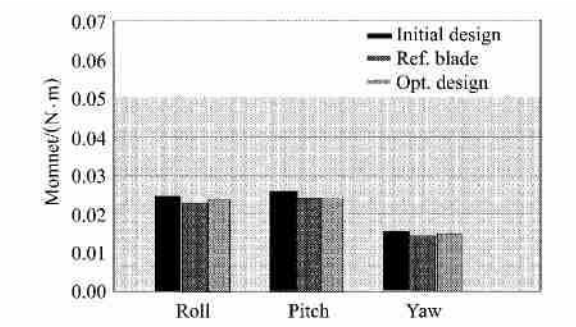


Fig. 5 3/rev hub moment (non-dimensional)

Fig. 6 and Fig. 7 give the comparisons of flapping and lead-lag stiffness, respectively, while the influence of swept angle to hub load is shown in Fig. 8.

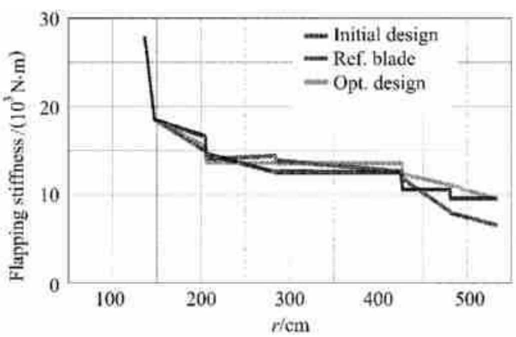


Fig. 6 comparison of blade flapping stiffness

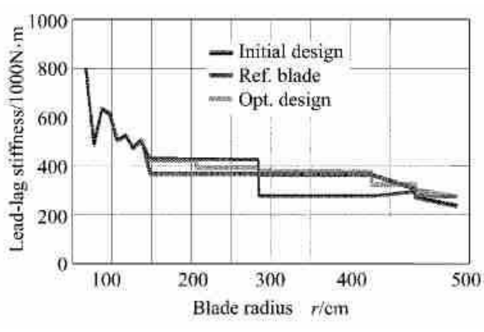


Fig. 7 Comparison of blade lead-lag stiffness

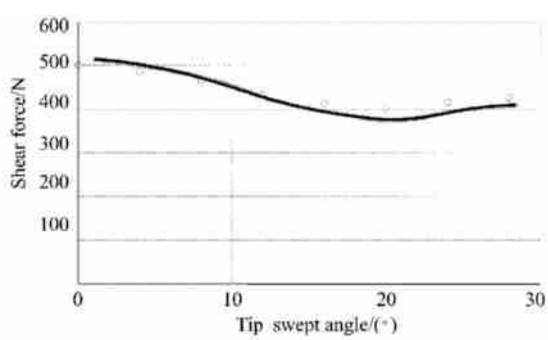


Fig. 8 Effect of tip swept angle on hub vertical shear

## 4 Concluding Remarks

A structural optimization of composite rotor blade with swept tip has been conducted. Numerical results for three-bladed rotor with C-spar and D-shape torsion box blade section are obtained. The following conclusions can be summarized based on the results studied in this configuration:

(1) The effect of structural parameter optimization by aeroelastic tailoring with composite ply organization has been demonstrated to minimize the $N$/rev vibratory hub load, while the lead-lag stiffness has larger potential for reduction of vibratory hub vertical shear force.

(2) The blade tip sweep angle has remarkable potential effect on hub vertical shear force, and a reasonable tip swept angle may result in great decrease in vibratory hub load. But be aware of that the instability margin might also decrease due to the increase of swept angle.

(3) The combined optimization effects of swept tip and composite ply structure are better than that of individuals.

(4) The combined sum of the hub shear force and moment components is a better objective function than the 3/rev hub vertical shear force alone, for the reduction effect of the other components is small; besides, the effect of ply with coupling is better than that of the uncoupled plys. This will be the future subject.

## References

[1] 向锦武, 郭俊贤, 张晓谷. 直升机减振的旋翼桨叶优化设计研究综述[J]. 北京航空航天大学学报, 2001, 27(1): 32-35.
Xiang J W, Guo J X, Zhang X G. An overview of rotor blade optimum design for helicopter vibration reduction [J]. Journal of Beijing University of Aeronautics and Astronautics, 2001, 27(1): 32-35. (in chinese)

[2] Yuan K A, Friedmann P P. Structural optimization for vibratory loads reduction of composite helicopter rotor blades with advanced geometry tips[J]. Journal of AHS, 1998, 43(3): 246-256.

[3] Kosmatka J B. Structural dynamic modeling of advanced composite propellers by the FEM [D]. Los Angeles: University of California, 1986.

[4] Giavotto V, Borri M, Mantegazza P, *et al*. Anisotropic beam theory and applications[J]. Computers and Structures, 1983, 16(1-4): 403-413.

[5] Refield L W. Design analysis methodology for composite rotor blades[J]. AIAA J, 1982, 20(5): 693- 699.

[6] Ganguli R, Chopra I. Aeroelastic optimization of an advanced geometry helicopter rotor[J]. Journal of AHS, 1996, 42(1): 18- 28.

[7] Ganguli R, Chopra I. Aeroelastic optimization of a helicopter rotor to reduce vibration and dynamic stresses[J]. Journal of Aircraft, 1996, 12(4): 808- 815.

[8] Adelman H M, Mantay W R. Integrated multidisciplinary design optimization of rotorcraft[J]. Journal of Aircraft, 1991, 28(1): 22- 28.

## Biographies:

**GUO Jun-xian** Born in August 1966, a senior engineer of helicopter at Chinese Helicopter Design and Development Institute. He received a B. Sc. in Engineering Mechanics from Northwestern Polytechnical University in 1989, a M. E. in aircraft design from Beijing University of Aeronautics and Astronautics(BUAA) in 2000. He is now a Ph. D. Candidate of BUAA. His research interests include helicopter design and composite structural design. He is an author of over 10 papers and has won 3 times award from the state and various ministries.

**XIANG Jin-wu** Born in April 1964, a professor of Aircraft Design at Beijing University of Aeronautics and Astronautics. He received B. Sc. and Ph. D. in Aircraft Design from Nanjing University of Aeronautics and Astronautics in 1984 and 1993, respectively, an M. E. in Engineering Mechanics from Northwestern Polytechnical University in 1990, and a in Aircraft Design from Nanjing University of Aeronautics and Astronautics in 1993. Dr. Xiang joined the faculty at Beijing University of Aeronautics and Astronautics in 1995, where he has been actively involved in teaching and research. He has been working on problems associated with aircraft design and aeromechanics of helicopters. He is an author of over 60 papers and has won 6 times award for promotion of science and technology from the state and various ministries.